RAA 2016 Vol. **16** No. **7**, 116 (10pp) doi: 10.1088/1674–4527/16/7/116
http://www.raa-journal.org *http://iopscience.iop.org/raa*

***R**esearch in*
***A**stronomy and*
***A**strophysics*

The influence of ionospheric thin shell height on TEC retrieval from GPS observation

Xiao-Lan Wang[1,2], Qing-Tao Wan[1], Guan-Yi Ma[1,2], Jing-Hua Li[1] and Jiang-Tao Fan[1]

[1] National Astronomical Observatories, Chinese Academy of Sciences, Beijing 100012, China; *guanyima@nao.cas.cn*
[2] University of Chinese Academy of Sciences, Beijing 100049, China

Received 2016 February 26; accepted 2016 March 26

Abstract We investigate the influence of assumed height for the thin shell ionosphere model on the Total Electron Content (TEC) derived from a small scale Global Positioning System (GPS) network. TEC and instrumental bias are determined by applying a grid-based algorithm to the data on several geomagnetically quiet days covering a 10 month period in 2006. Comparisons of TEC and instrumental bias are made among assumed heights from 250 km to 700 km with an interval of 10 km. While the TEC variations with time follow the same trend, TEC tends to increase with the height of the thin shell. The difference in TEC between heights 250 km and 700 km can be as large as ~ 8 TECU in both daytime and nighttime. The times at which the TEC reaches its peak or valley do not vary much with the assumed heights. The instrumental biases, especially bias from the satellite, can vary irregularly with assumed height. Several satellites show a large deviation of ~ 3 ns for heights larger than 550 km. The goodness of fit for different assumed heights is also examined. The data can be generally well-fitted for heights from 350 km to 700 km. A large deviation happens at heights lower than 350 km. Using the grid-based algorithm, there is no consensus on assumed height as related to data fitting. A thin shell height in the range $350 - 500$ km can be a reasonable compromise between data fitting and peak height of the ionosphere.

Key words: Radiowave propagation — Ionospheric TEC — Ionospheric height — GPS observation — Instrumental bias

1 INTRODUCTION

The ionosphere is a dispersive medium that causes a phase rotation or time delay in transionospheric radio waves used for radio astronomy and satellite navigation. The time delay of a radio wave propagating through the ionosphere is proportional to the Total Electron Content (TEC) along its ray path. Measurement of TEC is useful for ionospheric correction in a transionospheric radio system (Arikan et al. 2003; Lanyi & Roth 1988; Klobuchar 1989; Xue et al. 2015; Wang et al. 2014).

Since the Global Positioning System (GPS) was opened up for public usage, the ionospheric TEC has been measured with dual frequency GPS receivers economically and effectively. GPS TEC has become the most used parameter in studying ionospheric properties, constructing ionospheric models and making ionospheric corrections (Saito et al. 1998; Mendillo 2006; Kumar et al. 2014; Erickson et al. 2001; Xiong et al. 2014; Shim et al. 2008, 2010; Shim et al. 2014; Maruyama et al. 2004). Unfortunately, a GPS signal contains an additional delay due to instrumental bias that originates from hardware in the GPS satellite and the receiver. The difference between the instrumental delays in two signals can be referred to as instrumental or differential code bias and greatly restricts the accuracy of TEC estimation. Several techniques have been developed to determine these biases for accurate TEC derivation that can be applied to a single GPS receiver or small-scale, regional and global GPS networks (Lanyi & Roth 1988; Sardon et al. 1994; Otsuka et al. 2002; Coco et al. 1991; Rideout & Coster 2006; Arikan et al. 2008; Ma & Maruyama 2003; Themens et al. 2013; Choi et al. 2011; Li et al. 2015).

In the retrieval of TEC from dual-frequency GPS observations, the ionosphere is usually modeled as a thin shell where all the electrons are condensed. The assumed height of the ionosphere plays an important role in converting the vertical TEC (referred to as TEC in the following) from slant TEC due to the height dependence of the mapping function or the oblique-to-zenithal factor. The thin shell height is generally taken to be in the range 350 to 500 km (Coco et al. 1991; Mannucci et al. 1998; Arikan et al. 2008; Jin et al. 2012; Zhang et al. 2014; ćepni et al. 2013). Since the characteristics of the ionosphere vary with time and space, an assessment of the assumed height of the ionosphere has been a difficult task. Using simultaneous ver-

tical and slant TEC observations with a GPS receiver in Lancaster, England (53.9°N, 2.8°W), the thin shell height is determined from the linear gradient between the vertical TEC and the slant TEC. It is suggested that the shell height would be better placed in the range 600 km to 1200 km (Birch et al. 2002). The validity of the ionospheric height of 350 km was examined in the low-latitude and equatorial sector of India. With ionosonde observations, the peak height of the F layer varied from 275 km to 575 km. However, determination of the ionospheric height employing the inverse method suggested by Birch et al. (2002) did not obtain consistent results, especially for low elevations, but varied from a few hundred to one thousand kilometers and beyond in those regions of India. It was found that vertical TEC did not change significantly with height ranging from 250 km to 750 km as long as the elevation angle of the satellite was greater than 50 degrees (Rama Rao et al. 2006). An evaluation of the errors inherent in the thin shell model of the ionosphere found that an RMS of 1 TECU could be obtained with a 400 km height if the satellite elevation was restricted to 15 degrees or more (Smith et al. 2008).

Recently, numerical simulation was performed on the ionosphere to investigate the influence of the ionospheric height on the thin shell model by testing in the central and northern parts of South America. The TEC and the slant TEC were calculated by integrating the electron density from the NeQuick model along the line of sight. The converted vertical TEC from slant TEC was compared with the TEC for different heights from 350 km to 550 km in steps of 25 km. The results showed that a unique ionospheric height that reduces the conversion error to zero (i.e., transition over slant to vertical TEC) does not exist in the studied region (Brunini et al. 2011). With GPS and ionosonde observations from the Canadian High Arctic Ionospheric Network (CHAIN), Themens et al. (2013) investigated the effect of the thin shell height on instrumental bias. The bias estimation has a linear relationship with shell height sensitivity, which varies seasonally and with the solar cycle. Nevertheless, the shell height is taken to be 400 km at solar maximum and is adjusted to 350 km for solar minimum. These studies show that a consensus on assumed height has not been reached. They highlight the need to understand the impact of the assumed height for the ionosphere on derivation of TEC and bias estimation.

In this paper, we seek to examine the influence of the height of the thin shell ionosphere on TEC derivation with observations from a small scale GPS network. We aim to clarify the characteristics of TEC variation with height of the ionosphere and evaluate the accuracy of the algorithm for different heights. Section 2 briefly derives the algorithm used for calculating the TEC and instrumental bias associated with GPS observation. Section 3 displays the estimated TEC and instrumental bias for different assumed heights. A comparison is made of the TEC and instrumental bias for different heights. A comparison is also made among the goodness of fit to the observational data for different heights. Section 4 discusses the results and implications. Finally the conclusions are given in Section 5.

2 GPS OBSERVATION AND TEC EXTRACTION

The GPS data are from four dual-frequency GPS receivers located at Fuzhou (26.1°N, 119.1°E), Xiamen (24.5°N, 118.1°E), Guangzhou (23.1°N, 113.2°E) and Nanning (22.8°N, 108.3°E), which form a small scale network in southeast China. The network covers a region with $\sim 11^\circ$ and $\sim 3^\circ$ in longitude and latitude, respectively (Ma et al. 2014).

A GPS satellite transmits signals at frequencies $f_1 = 1575.42\,\mathrm{MHz}$ and $f_2 = 1227.60\,\mathrm{MHz}$. For a dual-frequency GPS receiver, the basic observations are two pseudoranges P_1 and P_2 resulting from group delay, and two measurements of phase advance, L_1 and L_2, corresponding to f_1 and f_2 respectively. The slant TEC along the path from satellite to receiver can be calculated as

$$N_{\mathrm{Tg}} = \frac{2(f_1 f_2)^2}{k(f_1^2 - f_2^2)}(P_2 - P_1), \tag{1}$$

$$N_{\mathrm{Tp}} = \frac{2(f_1 f_2)^2}{k(f_1^2 - f_2^2)}(L_1\lambda_1 - L_2\lambda_2), \tag{2}$$

where $k = 80.62\ \mathrm{m^3\ s^{-2}}$, and λ_1 and λ_2 are the wavelengths corresponding to f_1 and f_2, respectively. To reduce the effects of the pseudorange error on TEC, a baseline or offset denoted by B_{rs} between N_{Tg} and N_{Tp} can be used to obtain an absolute slant TEC with higher precision (Horvath & Essex 2000; Mannucci et al. 1998)

$$N_{\mathrm{T}} = N_{\mathrm{Tp}} + B_{\mathrm{rs}}. \tag{3}$$

For one continuous tracking arc with $\mathrm{M_{SR}}$ observation epochs, the B_{rs} is computed as the average between the pseudorange derived $N_{\mathrm{Tg}i}$ and phase derived $N_{\mathrm{Tp}i}$ over the index i from $i = 1$ to $i = \mathrm{M_{SR}}$ inclusive

$$B_{\mathrm{rs}} = \frac{\sum_{i=1}^{\mathrm{M_{SR}}}(N_{\mathrm{Tg}i} - N_{\mathrm{Tp}i})\sin^2\alpha_i}{\sum_{i=1}^{\mathrm{M}}\sin^2\alpha_i}, \tag{4}$$

where α_i is the elevation of the satellite. The $\sin^2\alpha_i$ is included as a weighting factor, since the pseudorange with low elevation is apt to be affected by the multipath such that the reliability decreases (Ma & Maruyama 2003).

For the ionosphere that is modeled as a thin shell at height h from Earth, as shown in Figure 1, the TEC at the piercing point P can be calculated from the following relation

$$N_{\mathrm{T}}^V = (N_{\mathrm{T}} - b_{\mathrm{s}} - b_{\mathrm{r}})\cos\chi, \tag{5}$$

with b_{s} and b_{r} being the instrumental biases of the satellite and receiver, respectively. $\cos\chi$ is the mapping function or the oblique-to-zenithal factor. χ is the zenith at the piercing

point which is related to satellite elevation and thin shell height

$$\chi = \arcsin\Big(\frac{\mathrm{R}_e \cos\alpha}{\mathrm{R}_e + h}\Big). \quad (6)$$

Another thin shell is also plotted in Figure 1. It can be seen that for a larger height of h_2, the zenith χ_2 is smaller than χ and hence $\cos\chi_2$ is larger than $\cos\chi$.

In this study, a grid-based algorithm is proposed for analyzing the small scale GPS network, which is used to determine the TEC and instrumental bias (Ma et al. 2014). The principle is briefly described in the following. The ionosphere over the small scale network is divided into 60 grid blocks in the region ($19°\mathrm{N} - 31°\mathrm{N}, 103.5°\mathrm{E} - 124.5°\mathrm{E}$). Each grid block is $1°$ by $3.5°$ in latitude and longitude, respectively. The TEC is assumed to be identical at any point within one grid block. The instrumental bias is taken as invariant within one day. For the line of sight from satellite j to receiver k piercing through the ionosphere in grid block m at time t, referring to Equation (5) and putting the unknowns on the left side, we can obtain the following equation

$$\sec\chi_{jk} N_{Ti}^V + b_{sj} + b_{rk} = N_{Tjk}, \quad (7)$$

where i denotes the order of the measurement and is related to the serial number of grid block m and time t. With $J(31)$ satellites and $K(4)$ receivers, to derive the TEC with a 15 min resolution, an overdetermined set of linear equations for $M(60)$ grid blocks can be written in matrix notation as the following:

$$\begin{bmatrix} \dots & \dots & \dots & \dots & \dots & \dots & \dots \\ \dots & \dots & \dots & \dots & \dots & \dots & \dots \\ \dots & \sec(\chi_{jk}) & \dots & 1 & \dots & 1 & \dots \\ \dots & \dots & \dots & \dots & \dots & \dots & \dots \\ \dots & \dots & \dots & \dots & \dots & \dots & \dots \end{bmatrix} \begin{bmatrix} N_{T1}^V \\ \cdot \\ \cdot \\ N_{TI}^v \\ b_{s1} \\ \cdot \\ \cdot \\ b_{sJ} \\ b_{r1} \\ \cdot \\ \cdot \\ b_{rK} \end{bmatrix} = \begin{bmatrix} \cdot \\ \cdot \\ N_{Tjk} \\ \cdot \\ \cdot \end{bmatrix} \quad (8)$$

where for N_{Ti}^V, $I = 96M$, since there are 96 TEC values each day for each grid block. $i = 1 + 96m, 2 + 96m, ..., 96 + 96m$ is for the TEC in grid block m. Moreover, a cutoff elevation of $30°$ is applied in the algorithm. It is preferable to take high elevation to suppress possible error caused by the assumed height in the mapping function. The selection of $30°$ is a compromise between data quantity and noise. With data from the small scale GPS network, there are 5795 $(96M + J + K)$ unknowns. For an assumed height of 400 km, the number of equations is $\sim 50\,000$ with a cutoff elevation of $30°$ in one day. With a least-squares fitting technique, the solution to the set of equations is obtained by singular value decomposition (SVD). The algorithm was implemented with Matlab following the above description.

3 TEC AND INSTRUMENTAL BIAS UNDER DIFFERENT ASSUMED HEIGHTS

The data were from four geomagnetically quiet days around equinoxes and solstices during a low solar activity phase in the year 2006. The days selected were 5 March, 24 June, 10 September and 26 December. TEC and instrumental biases are determined by applying the grid-based algorithm to the data obtained on the four days.

3.1 General Aspects

Setting a height of 450 km, the derived TECs over Fuzhou are shown in Figure 2. TECs from the Center for Orbit Determination in Europe (CODE, *ftp://ftp.unibe.ch/aiub/CODE*) are also plotted for comparison. Even though the difference between the grid-based and CODE TECs can be as large as 9 TECU in September, the overall trend in TEC variation remains similar for all the seasons. The variation in TECs shows a high degree of uniformity. TEC reaches its midday maximum at ~ 1500 local time (LT) and its minimum at ~ 0600 LT. As shown with a scatter plot in Figure 3, the retrieved satellite biases and those obtained from CODE are also compared. A diagonal line is drawn to indicate visually that the two biases derived independently agree with each other.

It should be pointed out that the TEC from the grid-based algorithm of this paper does not totally agree with that from CODE, since the algorithms are different and there are no GPS observations from Fuzhou to Nanning used in the CODE method. Arikan et al. (2003) compared TECs obtained from eight different methods (including those from CODE and other models). They showed that none of the methods were in agreement with one another. It is not useful to make an absolute comparison until a standard TEC measurement is available.

3.2 TEC Variation with Assumed Height

Under an assumed height from 250 km to 700 km with a step of 10 km, TEC and instrumental bias are determined by applying the grid-based algorithm to the data acquired on the four days. Figure 4 shows the retrieved TEC over Fuzhou at heights 250, 400, 550 and 700 km. The TEC tends to increase with the assumed height of the thin shell. The TEC increment is different for different times within one day and in different seasons. It is larger in spring and summer than in autumn and winter. The difference in TEC at a height between 250 and 700 km can be as large as ~ 8 TECU in both daytime and night. It is ~ 2 TECU between those from heights with an interval of 150 km. The variation of TEC with time at different thin shell heights is basically the same. The times at which the TEC reaches its peak or valley do not vary much with the assumption on height. It should be noted that in summer and autumn days, the dependence of TEC on assumed height can be irregular from morning to late evening. We can also occasion-

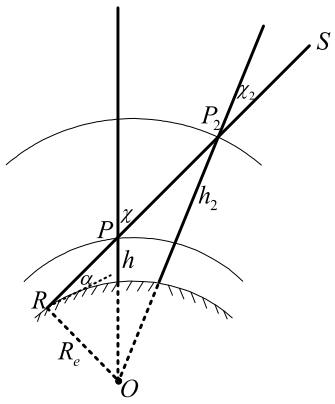

Fig. 1 Geometry of the thin shell ionosphere at height h from the Earth. Another thin shell is also drawn to show a larger height h_2 which leads to a smaller zenith angle χ_2.

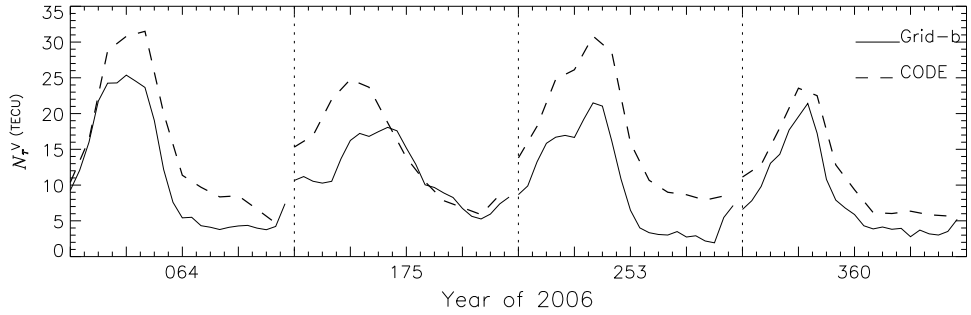

Fig. 2 The retrieved TEC at Fuzhou for four days covering a time span of 10 months. The TEC provided by CODE is also shown for comparison.

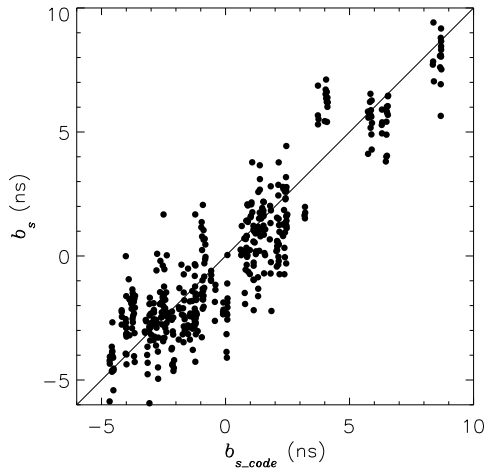

Fig. 3 A scatter plot of the retrieved satellite biases compared to those obtained by CODE.

ally find irrational values of TEC. On day 175, there are unreasonable values of TEC at $\sim 1600 - 1800$ UT for the heights 550 and 700 km. Actually, the unreasonable values of TEC start to appear from height 500 km. Although not shown in the paper, similar characteristics of TEC dependence on height are also observed at Xiamen, Guangzhou and Nanning. Unreasonable values of TEC also exist but at different times in both summer and winter.

Figure 5 shows the estimated instrumental biases of the 31 GPS satellites. Shown here is the relative bias, referring to the bias with the mean of the day being removed. The instrumental bias varies with height without a certain

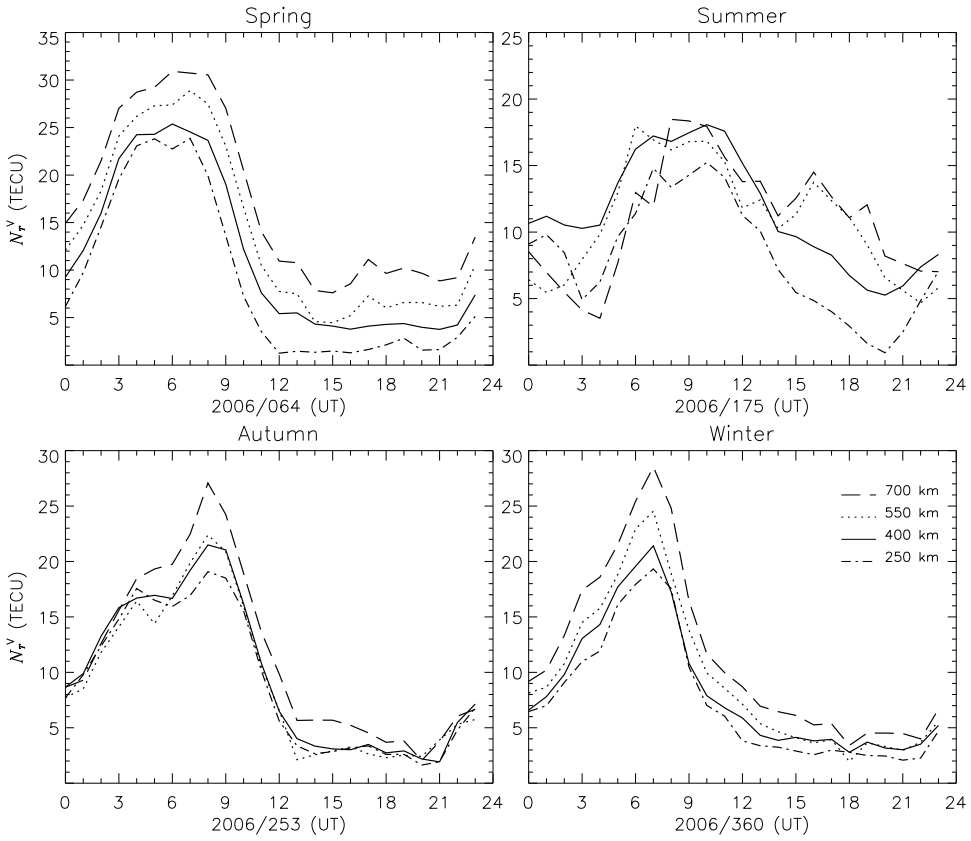

Fig. 4 The derived TEC at Fuzhou for assumed heights of 250, 400, 550 and 700 km.

trend for all satellites. The largest variation happens on day 175, which is the same day that gave unreasonable values of TEC. For satellite with a pseudo-random noise (PRN) number of 6, a difference of $\sim$ 7 ns can be found between 250 km and 700 km. Several satellites show a large deviation of $\sim$ 3 ns for a height of 700 km compared to other heights. PRN 2, PRN 10 and PRN 29 show the largest difference in bias between heights 250 km and 550 km. The difference on the other days is generally small with the smallest value being $\sim$ 0.5 ns. Figure 6 shows the receiver bias. The receiver bias tends to decrease or increase with height, with different behaviors on different days. The largest difference between assumed height happens on day 175. The smallest one happens on day 360. These are $\sim$ 1.5 ns and $\sim$ 0.1 ns which correspond to the largest and smallest differences, respectively. Both are much smaller than those of satellites.

Goodness of fit is a measure of how well the estimated parameters agree with the data. It is defined as the standard deviation of data from the estimated parameters (Bevington 1969).

$$\chi_g = \sqrt{\frac{\sum_{i=1}^{\mathrm{L}} (N_{Tjk} - \sec\chi_{jk} \cdot N_{Ti}^V - b_{sj} - b_{rk})^2}{(L - L_u)}}, \quad (9)$$

where L is the number of equations in Equation (8) and L_u is the number of unknowns plus one $(96M + J + K + 1)$.

Table 1 The Goodness of Fit for Different Heights

Height (km)	Day of the Year 064	175	253	360
250	0.84	1.78	0.96	0.85
400	0.65	1.47	0.75	0.62
550	0.66	1.48	0.79	0.56
700	0.67	1.34	0.68	0.55

Table 1 shows the goodness of fit at heights 250, 400, 550 and 700 km. The χ_g is largest for each height on day 175, indicating the fitting to the data is worst compared with those on other days. The largest difference is 0.44 TECU at heights between 250 and 700 km on day 175.

Figure 7 shows the goodness of fit corresponding to different assumed heights. Here, χ_g is normalized by its largest value and plotted in a range [min, max] on each day. Although different on each day, the largest χ_g happens for height 250 km for all days. From Figure 7, the goodness of fit is different for different heights. The fitting is usually good when the height is taken from 350 km to 700 km. Although seen to be large in Figure 7, for a height larger than 350 km, the largest difference in χ_g is $\sim$ 0.24 TECU on day 175, and the smallest difference of χ_g is 0.04 TECU on day 64. There can be several minimal values of χ_g. The smallest minimal value is different for different days. There is not a consensus about the assumed

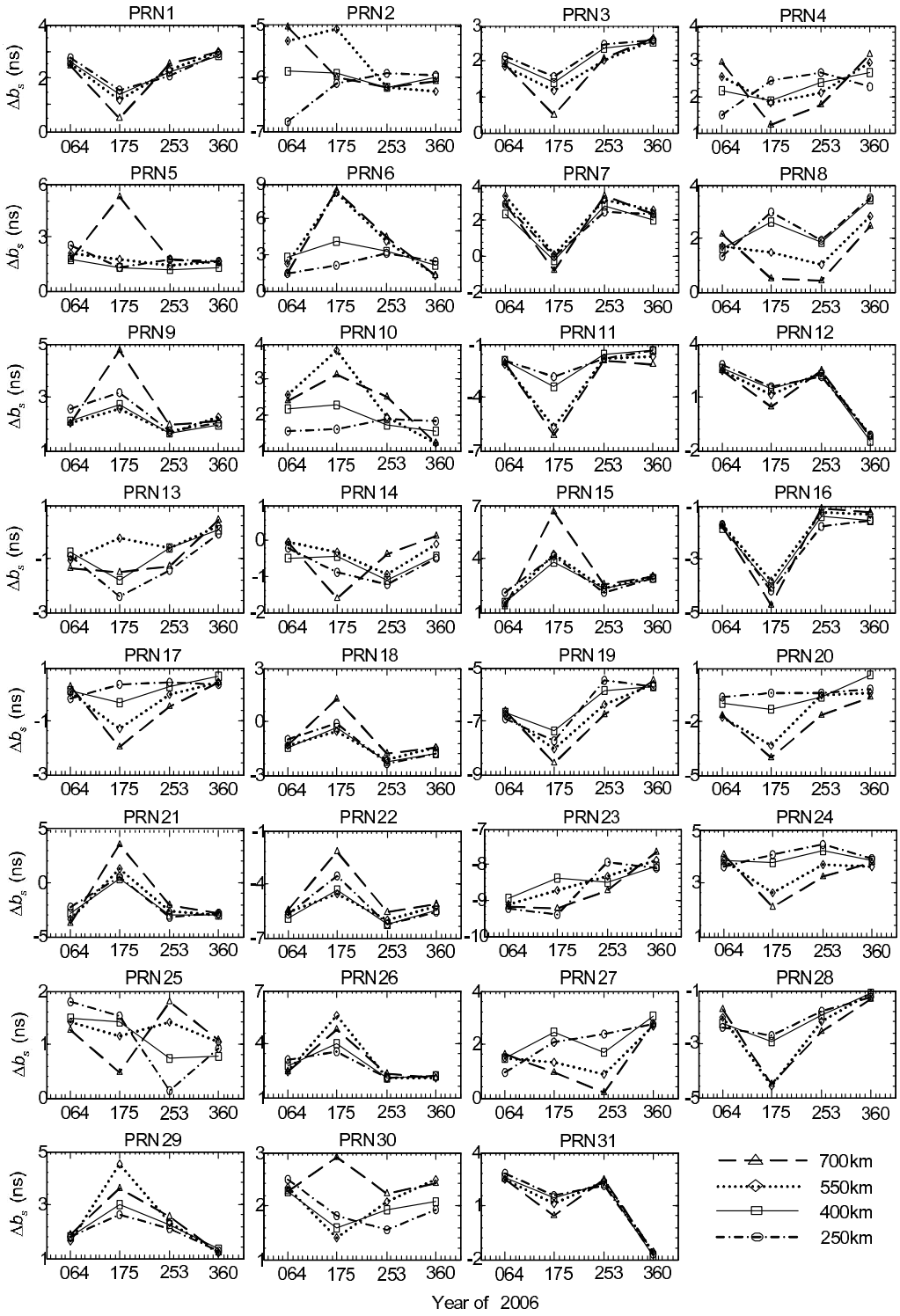

Fig. 5 The derived satellite bias on four days covering a 10 month time span in 2006, corresponding to heights 250, 400, 550 and 700 km. Shown here is the relative bias, referring to the bias with the mean of the day being removed.

height for all days that fitting is applied. The worst one happens at 250 km. Large deviations at heights lower than 350 km can be observed for all days. The goodness of fit becomes worse monotonically when the height decreases from 280 km to 250 km.

In order to understand the difference in TEC, instrumental bias and goodness of fit for different assumed heights, we should check the influence of the assumed height on the amount of data. Figure 8 shows the amount of data in the top right corner of each individual plot corre-

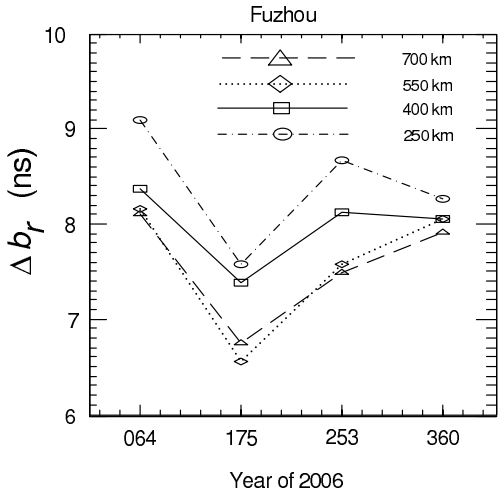

Fig. 6 The derived receiver bias. Shown here is the relative bias.

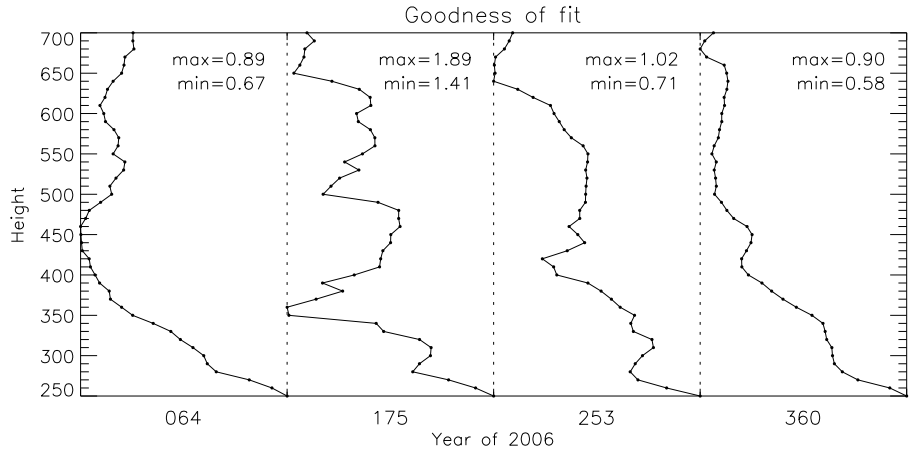

Fig. 7 Height profile features of the normalized goodness of fit χ_g on each day. The horizontal scale ranges within [min, max].

sponding to 250, 400, 550 and 700 km. Plotted as a horizontal bar, the data are categorized into six groups by elevation: $30^\circ - 40^\circ$, $40^\circ - 50^\circ$, $50^\circ - 60^\circ$, $60^\circ - 70^\circ$, $70^\circ - 80^\circ$, and $80^\circ - 90^\circ$. The horizontal scale is 16 194, which corresponds to the amount of data within elevation $30^\circ - 40^\circ$ on day 360 for $h = 250$ km. Although the amount of data is different on different days, the distribution of elevation for the data is similar on different days. For $h = 250$ km, the percentage of the data for $30^\circ - 40^\circ$ is about 26%, as is that for $40^\circ - 50^\circ$. The percentage of data for $50^\circ - 60^\circ$ is about 21%. The percentage of data for $60^\circ - 90^\circ$ is about 24%. Compared with that for 250 km, a decrease in the amount of data happens at a low elevation of $30^\circ - 40^\circ$ for 400 km. Considerable loss happens for $30^\circ - 40^\circ$ and a small part happens at $40^\circ - 50^\circ$ for 550 km. The amount of data with an elevation of $50^\circ - 60^\circ$ can be seen to decease for 700 km. Moreover, considerable loss happens for $40^\circ - 50^\circ$ and only a small part of $40^\circ - 50^\circ$ is left. With an increase in the assumed height, the lines of sight with low elevations tend to be unbounded from the grid block, so that the amount of data used for TEC derivation decreased.

4 DISCUSSION

Most of the TEC contribution comes from electrons at the peak height of the ionosphere where the electron density of the ionosphere is maximum. There are more electrons in the higher part of the ionosphere than in the lower part. This indicates that the height of the thin shell should be larger than the height of the ionospheric peak. The typical height of the ionospheric peak is ~ 300 km at low latitude during a low phase in solar activity (Rama Rao et al. 2006; Hoque & Jakowski 2012). In this study, the trend of TEC increases with the assumed height. This is reasonable because the vertical TEC is linearly related to the mapping function $\cos\chi$ which increases with height. The difference in TEC can be as large as ~ 8 TECU on days 64 and 175 for assumed height between 250 km and 700 km, though it is smaller on days 253 and 360. The difference in TEC is ~ 2 TECU for an assumed height between 400 km and

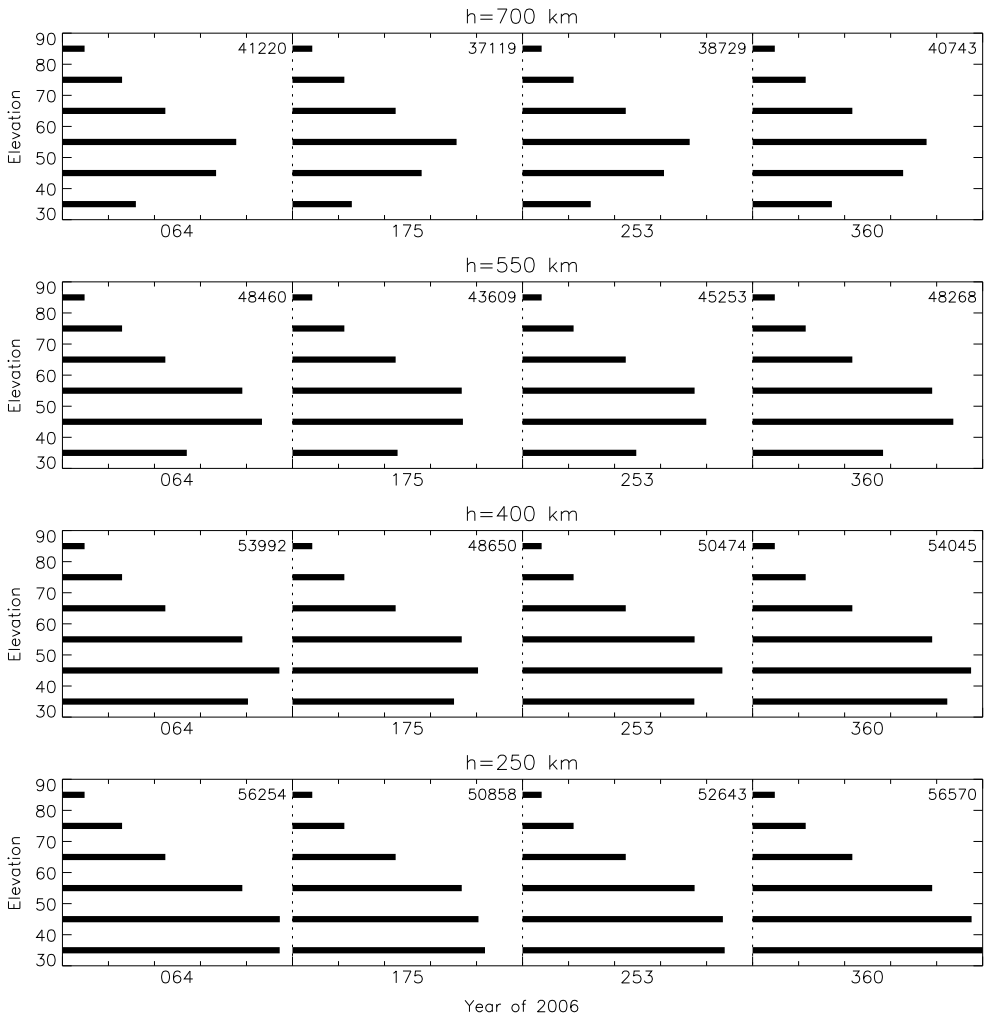

Fig. 8 The amount of data corresponding to elevation ranges of $30^\circ - 40^\circ$, $40^\circ - 50^\circ$, $50^\circ - 60^\circ$, $60^\circ - 70^\circ$, $70^\circ - 80^\circ$, and $80^\circ - 90^\circ$ for different assumed heights. Shown in the top right corner of each graph is the total number of data used for TEC derivation. The amount of data within $30^\circ - 40^\circ$ has the largest value of 16 194 on day 360 for $h = 250$ km, which is taken as the horizontal scale.

550 km. The behavior of the TEC variation with time is almost the same for different assumed heights. The goodness of fit is the worst on day 175. For all days, the worst goodness of fit happens for the assumed height of 250 km. A worse fit means the data are noisy, or the data deviate from one another. Considering that the lines of sight from different satellites converge to the grid block, the data from cases with smaller elevation tend to be more noisy. There is more data at elevation $30^\circ - 40^\circ$ at an assumed height of 250 km. This implies that the assumption of a uniform ionosphere tends to be contradicted in the grid block at a height lower than the true thin shell height, so the goodness of fit becomes worse.

With the increase of height from 250 km, the goodness of fit becomes better. It is significantly improved at height $\sim$ 450 km on day 64, $\sim$ 360 km on day 175, and 420 km on days 253 and 360. The goodness of fit is usually good for a height larger than 350 km for all days. Although on day 175 the χ_g becomes worse when height is larger than 360 km, it becomes better when height is larger than 400 km. A height larger than 400 km leads to appreciable χ_g on other days. There are several minimal values of χ_g each day. The smallest is different for different days. A best assumed height does not exist as related to data fitting. The amount of data used for derivation of TEC decreases with increase of the assumed height. Significant reduction of low elevation data happens for an assumed height larger than 400 km. This is because the lines of sight with low elevations at a grid block at lower height tend to be unrelated to a grid block at higher altitude. The data corresponding to larger height contain less noise than those from lower heights. Hence, a better χ_g tends to be obtained for a larger assumed height. However, the χ_g does not decrease (become better) monotonically with height for the range $350 - 700$ km. A good χ_g obtained for a lower assumed height tends to reflect the agreement between assumption and observation. We can speculate that the best assumed height is $\sim$ 450 km on day 64, $\sim$ 360 km on day 175,

and 420 km on days 253 and 360. There does not exist a consensus for height for all days. This is understandable considering that the ionosphere, including the peak height, varies all the time. Moreover, it is impossible to conclude there is a best assumed height with only GPS observations in this study. A thin shell height in the range $350 - 500$ km can be a reasonable compromise between data fitting and observation of ionospheric peak height. A model of thin shell height with diurnal variation is necessary for accurate TEC derivation from GPS observation. Recently, the ionospheric peak height model was studied (Zhang et al. 2009; Hoque & Jakowski 2012). Deviation of TEC from GPS observation would be improved by implementing the peak height model with the assumption of a thin shell ionosphere.

5 CONCLUSIONS

This paper studies the influence of the height of the thin shell model of the ionosphere on retrieval of TEC with a grid-based algorithm and GPS observations from a small scale network in a low latitude region. TEC and instrumental bias are derived by applying the algorithm to four geomagnetically quiet days selected from four seasons of 2006 in a low phase of solar activity. Comparisons of TEC and instrumental bias are made among assumed heights from 250 to 700 km with an interval of 10 km. The TEC variations with time follow the same trend. The times at which the TEC reaches its peak or valley do not vary significantly with assumed height. TEC tends to increase with height of the thin shell. At TEC maximum, it tends to increase ~ 1.8 TECU with a 100 km increase in assumed height. The difference in TEC at heights between 250 and 700 km can be as large as ~ 8 TECU at both daytime and night. At heights larger than 500 km, unreasonable values of TEC occur occasionally on day 175 in summer. The instrumental bias, especially the satellite bias, can change irregularly with height. Several satellites show large deviation of ~ 3 ns for heights larger than 550 km.

The goodness of fit to the GPS data is also examined for different heights. It has a large deviation at heights lower than 350 km because data tend to be more noisy when converting the vertical TEC from slant TEC due to lower elevation. The goodness of fit worsens monotonically in the range $250 - 280$ km. The fitting is generally good when the height is taken as $350 - 700$ km, though it varies randomly with height. Assumed height in the range $350 - 500$ km can be a reasonable compromise between data fitting and peak ionosphere height. A thin shell height model is necessary for accurate derivation of TEC from GPS observation.

Acknowledgements This work is supported by the National Natural Science Foundation of China (Grant Nos. 11473045, 11403045 and 11503040).

References

Arikan, F., Erol, C. B., & Arikan, O. 2003, Journal of Geophysical Research (Space Physics), 108, 1469
Arikan, F., Nayir, H., Sezen, U., et al. 2008, Radio Science, 43
Bevington, P. R. 1969, Data Reduction and Error Analysis for the Physical Sciences (New York: McGraw-Hill)
Birch, M., Hargreaves, J., & Bailey, G. 2002, Radio Science, 37
Brunini, C., Camilion, E., & Azpilicueta, F. 2011, Journal of Geodesy, 85, 637
ćepni, M. S., Potts, L. V., & Miima, J. B. 2013, Space Weather, 11, 520
Choi, B. K., Cho, J. H., & Lee, S. J. 2011, Advances in Space Research, 47, 1590
Coco, D. S., Coker, C., Dahlke, S. R., & Clynch, J. R. 1991, IEEE Transactions on Aerospace Electronic Systems, 27, 931
Erickson, W. C., Perley, R. A., Flatters, C., et al. 2001, A&A, 366, 1071
Hoque, M. M., & Jakowski, N. 2012, Annales Geophysicae, 30, 797
Horvath, I., & Essex, E. A. 2000, Journal of Atmospheric and Solar-Terrestrial Physics, 62, 371
Jin, R., Jin, S., & Feng, G. 2012, GPS solutions, 16, 541
Klobuchar, J. 1989, Modern Total Electron Content Measurement in World Ionosphere-Thermosphere Study, 2 (ICSU SCOSTEP)
Kumar, S., Tan, E. L., Razul, S. G., et al. 2014, Earth, Planets and Space, 66, 1
Lanyi, G. E., & Roth, T. 1988, Radio Science, 23, 483
Li, L. X., Zhang, D. H., Zhang, S. R., et al. 2015, Radio Science, 50, 339
Ma, G., Gao, W., Li, J., Chen, Y., & Shen, H. 2014, Advances in Space Research, 54, 871
Ma, G., & Maruyama, T. 2003, Annales Geophysicae, 21, 2083
Mannucci, A. J., Wilson, B. D., Yuan, D. N., et al. 1998, Radio Science, 33, 565
Maruyama, T., Ma, G., & Nakamura, M. 2004, Journal of Geophysical Research (Space Physics), 109, A10302
Mendillo, M. 2006, Reviews of Geophysics, 44
Otsuka, Y., Ogawa, T., Saito, A., et al. 2002, Earth, Planets, and Space, 54, 63
Rama Rao, P. V. S., Niranjan, K., Prasad, D. S. V. V. D., Gopi Krishna, S., & Uma, G. 2006, Annales Geophysicae, 24, 2159
Rideout, W., & Coster, A. 2006, GPS Solutions, 10, 219
Saito, A., Fukao, S., & Miyazaki, S. 1998, Geophys. Res. Lett., 25, 3079
Sardon, E., Rius, A., & Zarraoa, N. 1994, Radio Science, 29, 577
Shim, J. S., Scherliess, L., Schunk, R. W., et al. 2008, Journal of Geophysical Research (Space Physics), 113, A09309
Shim, J. S., Scherliess, L., Schunk, R. W., et al. 2010, Journal of Geophysical Research (Space Physics), 115, A04307
Shim, J. S., Kuznetsova, M., Rastätter, L., et al. 2014, Modeling the Ionosphere-Thermosphere System, 145

Smith, D. A., Araujo-Pradere, E. A., Minter, C., et al. 2008, Radio Science, 43

Themens, D. R., Jayachandran, P., Langley, R., MacDougall, J., & Nicolls, M. 2013, GPS solutions, 17, 357

Wang, C., Zhang, M., Xu, Z.-W., Mao, C., & Chen, C. 2014, Chinese J. Geophysics, 57, 3570

Xiong, B., Wan, W.-X., Ning, B.-Q., et al. 2014, Chinese Journal Geophysics, 57, 3586

Xue, J., Song, S., & Zhu, W. 2015, Scientia Sinica Physica, Mechanica & Astronomica, 45, 079505

Zhang, D.-H., Shi, Y., Jin, W., Zhang, W., Hao, Y., & Xiao, Z. 2014, Science China Technological Sciences, 57, 67

Zhang, M.-L., Liu, C., Wan, W., Liu, L., & Ning, B. 2009, Annales Geophysicae, 27, 3203